CX3CR1 is a gatekeeper for intestinal barrier integrity in mice: Limiting steatohepatitis by maintaining intestinal homeostasis.

HEPATOLOGY
Official Journal of the American Association for the Study of Liver Diseases

CX3CR1 Is a Gatekeeper for Intestinal Barrier Integrity in Mice: Limiting Steatohepatitis by Maintaining Intestinal Homeostasis

Kai Markus Schneider,[1*] Veerle Bieghs,[1*] Felix Heymann,[1] Wei Hu,[1] Daniela Dreymueller,[2] Lijun Liao,[1] Mick Frissen,[1] Andreas Ludwig,[2] Nikolaus Gassler,[3] Oliver Pabst,[4] Eicke Latz,[5,6,7] Gernot Sellge,[1] John Penders,[8] Frank Tacke,[1] and Christian Trautwein[1]

Nonalcoholic fatty liver disease is seen as the hepatic manifestation of the metabolic syndrome and represents the most common liver disease in Western societies. The G protein–coupled chemokine receptor CX3CR1 plays a central role in several metabolic syndrome–related disease manifestations and is involved in maintaining intestinal homeostasis. Because diet-induced intestinal dysbiosis is a driver for nonalcoholic fatty liver disease, we hypothesized that CX3CR1 may influence the development of steatohepatitis. In two independent models of diet-induced steatohepatitis (high-fat diet and methionine/choline-deficient diet), CX3CR1 protected mice from excessive hepatic steatosis and inflammation, as well as systemic glucose intolerance. Lack of *Cx3cr1* expression was associated with significantly altered intestinal microbiota composition, which was linked to an impaired intestinal barrier. Concomitantly, endotoxin levels in portal serum and inflammatory macrophages in liver were increased in *Cx3cr1*$^{-/-}$ mice, indicating an increased inflammatory response. Depletion of intestinal microbiota by administration of broad-spectrum antibiotics suppressed the number of infiltrating macrophages and promoted macrophage polarization in liver. Consequently, antibiotic-treated mice demonstrated a marked improvement of steatohepatitis. *Conclusion*: Microbiota-mediated activation of the innate immune responses through CX3CR1 is crucial for controlling steatohepatitis progression, which recognizes CX3CR1 as an essential gatekeeper in this scenario. (HEPATOLOGY 2015;62:1405-1416)

Nonalcoholic fatty liver disease covers a broad spectrum of diseases ranging from steatosis to nonalcoholic steatohepatitis (NASH). NASH is characterized by steatosis in combination with inflammation and can further progress to fibrosis and hepatocellular carcinoma.[1] NASH is associated with the metabolic syndrome, and due to the obesity epidemic, the incidence of NASH is rising dramatically.[2,3] However, not all obese people develop NASH and lean persons can also suffer from steatohepatitis,[4] indicating that additional causes, such as genetic and environmental factors, may be involved in the transition from steatosis to NASH.

Abbreviations: ALT, alanine aminotransferase; BMDM, bone marrow–derived macrophage; FACS, fluorescence-activated cell sorting; FKN, fractalkine; HFD, high-fat diet; Il1b/Il1β, interleukin 1-beta; MCD, methionine/choline-deficient; Mcp1, monocyte chemoattractant protein 1; NAS, nonalcoholic fatty liver disease activity score; NASH, nonalcoholic steatohepatitis; NCD, normal control diet; PAMP, pathogen-derived molecular pattern; TLR, toll-like receptor; WT, wild type.

From the [1]Department of Internal Medicine III, University Hospital, RWTH Aachen, Aachen, Germany; [2]Institute of Pharmacology and Toxicology, Medical Faculty, University Hospital, RWTH Aachen, Aachen, Germany; [3]Institute of Pathology, University Hospital, RWTH Aachen, Aachen, Germany; [4]Institute of Molecular Medicine, University Hospital, RWTH Aachen, Aachen, Germany; [5]Institute of Innate Immunity, University Hospital, University of Bonn, Bonn, Germany; [6]Department of Medicine, University of Massachusetts Medical School, Worcester, MA; [7]German Center for Neurodegenerative Diseases, Bonn, Germany; [8]Department of Medical Microbiology, School for Nutrition and Translational Research in Metabolism, Maastricht University Medical Center, Maastricht, The Netherlands

Received April 20, 2015; accepted July 9, 2015.

Additional Supporting Information may be found at onlinelibrary.wiley.com/doi/10.1002/hep.27982/suppinfo.

**These authors contributed equally to this work.*

Supported by a grant from the Alexander von Humboldt Foundation (3.3-BEL/1147960 STP), the German Research Foundation (DFG: BI 1670/2-1, TR 285/10-1; SFB/TRR57), the German Cancer Aid (Mildred-Scheel research scholarship: #110790), the Federal Ministry of Education and Research (ObiHep grant #01KU1214B) the Interdisciplinary Centre for Clinical Research (START grant #691438) within the Faculty of Medicine at the RWTH Aachen University, and the SFB 985, Project C3. [Correction added October 6, 2015, after first online publication: "SFB 985, Project C3" was added to the funding information.].

The chemokine receptor CX3CR1 (also known as GPR-13) has been linked to metabolic syndrome–related diseases, including diabetes,[5] obesity,[6] and atherosclerosis.[7,8] Due to cleavage of the extracellular domain, higher circulating levels of fractalkine (FKN) are linked to onset of the metabolic syndrome.[6] Interestingly, it is thought that intestinal barrier dysfunction as well as intestinal dysbiosis are also associated with these metabolic disorders.[9-11] Intestinal macrophages are defined by their expression of CX3CR1, and $MHCII^{hi}$ $CD11b^{+}CD11c^{+}F4/80^{+}CX3CR1^{hi}$ macrophages in the gut are critical for intestinal barrier integrity. These cells have a high phagocytic capacity and limit translocation of pathogen-derived molecular patterns (PAMPs) as well as microbiota-derived molecular patterns.[12,13] Recently, it has been demonstrated that *Cx3cr1*$^{-/-}$ mice have decreased numbers of these mucosal resident macrophages, show increased bacterial translocation to mesenteric lymph nodes, and have increased susceptibility to dextran sodium sulfate–induced colitis.[14] Moreover, CX3CR1 mediates direct protective effects on intestinal epithelial cells, including autocrine regulation of cell-survival signals and activation of immune modulators.[15]

During the pathogenesis of steatohepatitis, translocation of PAMPs plays a critical role in murine disease models.[16,17] Indeed, recent data indicate that also patients suffering from steatohepatitis have a disturbed intestinal barrier, suggesting an essential role of this mechanism in human disease manifestations.[18] The intestinal barrier is formed by a single layer of intestinal epithelial cells, which are interconnected by tight junctions and covered by mucus.[19] Therefore, loss of tight junctions as a result of intestinal dysbiosis facilitates gut leakiness and translocation of PAMPs to the liver. Increased numbers of PAMPs in the venous circulation of the gut can activate pathogen recognition receptors, such as Toll-like receptors (TLRs) and multiprotein inflammasome complexes and thereby trigger an inflammatory response that contributes to the development and progression of steatohepatitis.[20,21]

Here, we investigated how CX3CR1 regulates intestinal microbiome homeostasis and thereby influences diet-induced steatohepatitis. Our present work suggests that CX3CR1 is an essential gatekeeper in microbiota-mediated activation of the innate immune response and consequently progression of steatohepatitis.

Materials and Methods

Mouse Experiments. All animal experiments were approved by the appropriate German authorities (LANUV, North Rhine-Westphalia, Az 84-02.04. 2012.A260). All animals received humane care according to the criteria outlined in the "Guide for the Care and Use of Laboratory Animals" prepared by the National Academy of Sciences and published by the National Institutes of Health (publication 86-23, revised 1985). C57BL/6 wild-type (WT) and *Cx3cr1*-deficient (*Cx3cr1*$^{-/-}$) mice (C57BL/6 background) were housed in filter-top cages. The *Cx3cr1*$^{-/-}$ mice had green fluorescent protein inserted into the CX3CR1 genetic locus.[22] All experiments were performed in 6-week-old to 8-week-old male mice. Two different dietary models were used to induce steatohepatitis—16 weeks of 60% high-fat diet (HFD; WT n = 5 and CX3CR1$^{-/-}$ n = 4; D12492; Research Diet Services BV, Gentofte, Denmark) and 8 weeks of methionine/choline-deficient diet (MCD; WT n = 7 and CX3CR1$^{-/-}$ n = 6; 960439; MP Biomedicals, Heidelberg, Germany). A normal chow diet (NCD) was used as a control diet (both WT and *Cx3cr1*$^{-/-}$ mice n = 2).

Collection of blood and tissue specimens, biochemical determination of liver lipids, caspase 3 activity assay, RNA isolation, complementary DNA synthesis, quantitative polymerase chain reaction, and serum parameters (aminotransferases, glutamate dehydrogenase, and alkaline phosphatase) were determined as described.[23,24] Administration of broad-spectrum antibiotics, isolation of intestinal epithelial and lamina propria cells, oral glucose tolerance test, endotoxin measurement, histology, microbiota data analysis, fluorescence-activated cell sorting (FACS), immunoblotting, cell culture experiments, and statistical analysis are described in detail in the Supporting Information.

Results

Cx3cr1 Deletion Triggers Progression of Diet-Induced Steatohepatitis. To investigate the relevance of CX3CR1 for the progression of diet-induced steatohepatitis, we fed WT and *Cx3cr1*$^{-/-}$ mice two different

Address reprint requests to: Veerle Bieghs, Ph.D., Department of Internal Medicine III, University Hospital, RWTH Aachen, Pauwelsstraße, 30, Aachen 52074, Germany. E-mail: veerlebieghs@hotmail.com; tel: +0241-80-80662; fax: +0241-80-82455.

View this article online at wileyonlinelibrary.com.
DOI 10.1002/hep.27982
Potential conflict of interest: Nothing to report.

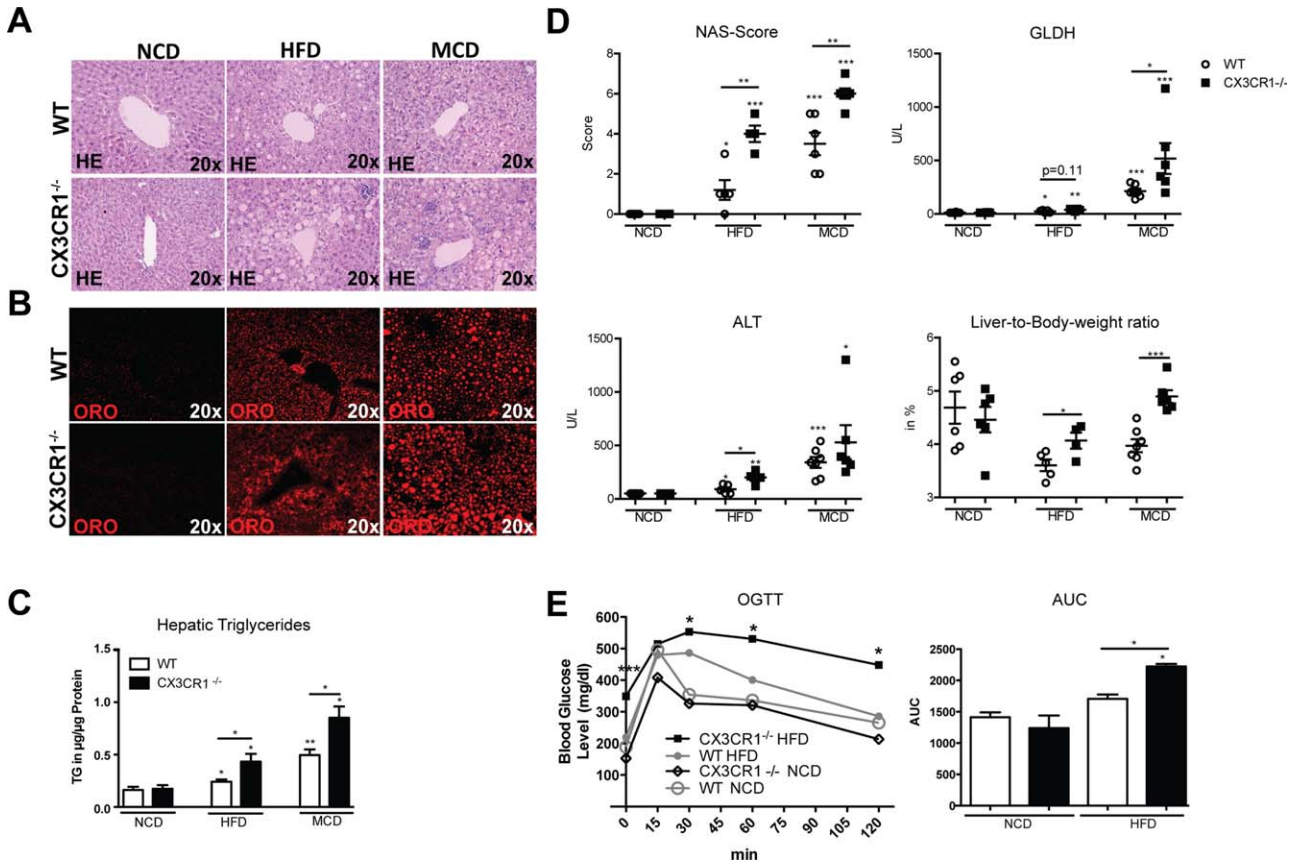

Fig. 1. Liver injury and glucose intolerance upon diet-induced steatohepatitis. (A) Hematoxylin and eosin staining, (B) oil red O staining, and (C) triglyceride levels in livers of WT and *Cx3cr1*$^{-/-}$ mice on NCD, HFD, and MCD. (D) NAS, serum glutamate dehydrogenase and ALT levels, and liver-to-body weight ratio in WT and *Cx3cr1*$^{-/-}$ mice on NCD, HFD, and MCD. (E) Oral glucose tolerance test and area under the curve after 0, 15, 30, 60, and 120 minutes. Data are expressed as the mean ± standard error of the mean and considered significant at $^{*}P < 0.05$, $^{**}P < 0.01$, and $^{***}P < 0.001$. *Significantly different from the resp. control group upon NCD, unless indicated differently. Abbreviations: AUC, area under the curve; GLDH, glutamate dehydrogenase; HE, hematoxylin and eosin; OGTT, oral glucose tolerance test; ORO, oil red O; TG, triglyceride.

experimental diets (HFD [16 weeks] and MCD [8 weeks] diet). HFD and MCD feeding induced more severe hepatic steatosis in *Cx3cr1*$^{-/-}$ compared to WT mice, evidenced by increased lipid accumulation shown by hematoxylin and eosin and oil red O staining (Fig. 1A,B) as well as hepatic triglyceride levels (Fig. 1C). In addition, *Cx3cr1*$^{-/-}$ mice had a higher histopathological nonalcoholic fatty liver disease activity score (NAS), higher serum levels of liver injury markers glutamate dehydrogenase and alanine aminotransferase (ALT), and a higher liver-to-body weight ratio (Fig. 1D). In contrast, the body weight did not differ between the groups (Supporting Fig. S1A).

Additionally, *Cx3cr1*$^{-/-}$ mice showed higher fasting glucose levels as well as decreased oral glucose tolerance in comparison to WT mice after HFD feeding but not to control fed mice (Fig. 1E). These data indicate that upon dietary challenge *Cx3cr1*$^{-/-}$ mice have impaired glucose metabolism.

The MCD diet furthermore induced increased cell death in livers of *Cx3cr1*$^{-/-}$ mice because we identified higher numbers of terminal deoxynucleotidyl transferase–mediated deoxyuridine triphosphate nick-end labeling–positive and cleaved caspase-3-positive cells (Supporting Fig. S2A), increased caspase-3 activity (Supporting Fig. S2B), as well as ballooning hepatocytes (Supporting Fig. S1D,E) compared to WT mice. In addition, sirius red staining revealed increased pericellular fibrosis upon MCD feeding in *Cx3cr1*$^{-/-}$ mice compared to WT mice (Supporting Fig. S2C). Expression of fibrosis-related genes such as collagen type 1 alpha 1 (*Col1a1*), transforming growth factor beta, and alpha-smooth muscle actin (Supporting Fig. S2D) was found to be increased after MCD diet in *Cx3cr1*$^{-/-}$ mice compared to WT mice. Altogether, these data indicate that lack of *Cx3cr1* expression results in more severe liver injury and is associated with systemic glucose intolerance upon diet-induced steatohepatitis in mice.

CX3CR1 Controls the Inflammatory Response During Diet-Induced Steatohepatitis. Next, we investigated the relevance of CX3CR1 for hepatic inflammation during diet-induced steatohepatitis.

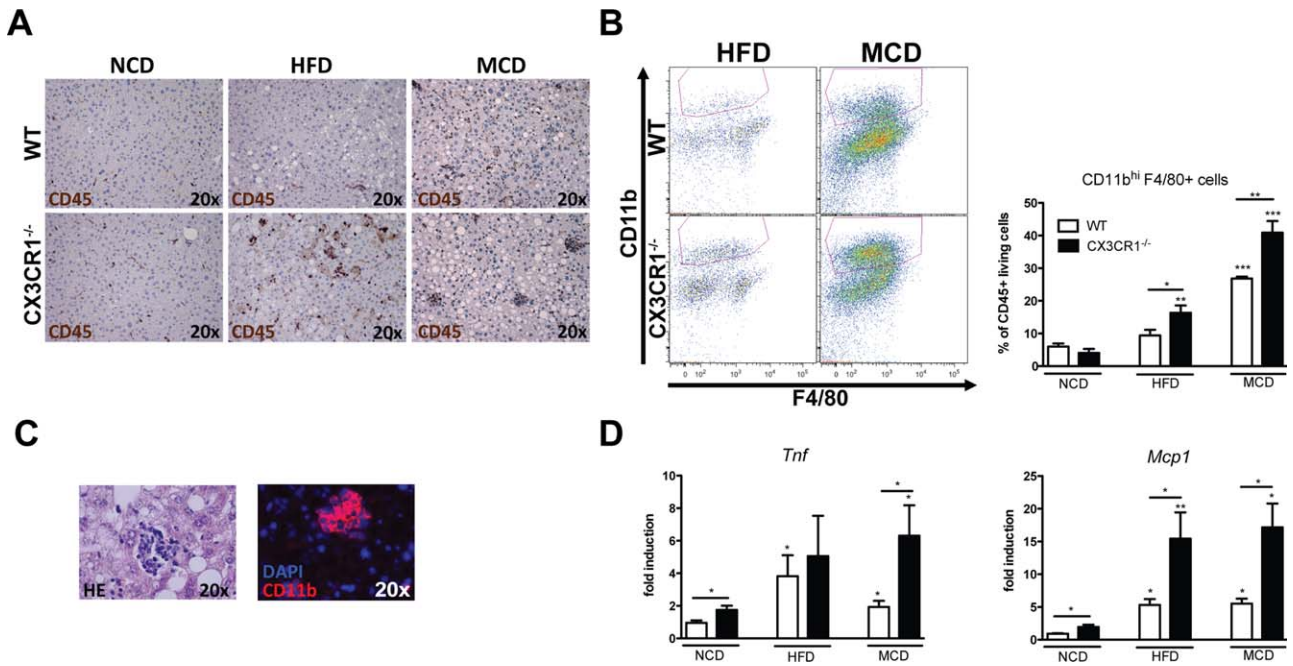

Fig. 2. Inflammatory responses in diet-induced liver injury. (A) Immunohistochemical staining against CD45 in livers of WT and *Cx3cr1*$^{-/-}$ mice on HFD and MCD. (B) Flow-cytometric analysis of infiltrating inflammatory macrophages (CD11b^{hi}F4/80^{low}) in livers of WT and *Cx3cr1*$^{-/-}$ mice on NCD, HFD, and MCD. (C) Hematoxylin and eosin and immunofluorescent staining against CD11b in livers of *Cx3cr1*$^{-/-}$ mice. (D) Hepatic gene expression of the proinflammatory cytokines tumor necrosis factor-alpha and monocyte chemoattractant protein 1 in WT and *Cx3cr1*$^{-/-}$ mice on NCD, HFD, and MCD. Data are expressed as the mean ± standard error of the mean and considered significant at $*P < 0.05$, $**P < 0.01$, and $***P < 0.001$. *Significantly different from the resp. control group upon NCD, unless indicated differently. Abbreviations: DAPI, 4′,6-diamidino-2-phenylindole; HE, hematoxylin and eosin; Mcp1, monocyte chemoattractant protein 1; *Tnf*, tumor necrosis factor-alpha.

Immunohistochemical staining against CD45 revealed more infiltration of immune cells in livers of *Cx3cr1*$^{-/-}$ mice compared to WT controls after both HFD and MCD (Fig. 2A). Additionally, FACS analysis demonstrated that inflammatory macrophages (defined as CD11b^{hi}F4/80^{low}) were the predominant infiltrating cell type (Fig. 2B). Immunostaining against CD11b in livers of *Cx3cr1*$^{-/-}$ mice revealed that these clusters of inflammatory cells were CD11b-positive (Fig. 2C).

Stronger immune cell infiltration in livers of *Cx3cr1*$^{-/-}$ mice was associated with higher gene expression of the proinflammatory cytokines tumor necrosis factor alpha and monocyte chemoattractant protein 1 (*Mcp1*) (Fig. 2D), which are known to aggravate steatohepatitis.[25] This difference was already apparent on NCD, indicating basal inflammatory differences between WT and *Cx3cr1*$^{-/-}$ mice. Hence, these data demonstrate that CX3CR1 is involved in limiting the inflammatory response during diet-induced steatohepatitis.

Alterations in Gut-Microbiota Composition of Cx3cr1*$^{-/-}$ *Mice. Steatohepatitis is associated with intestinal dysbiosis; therefore, we next analyzed the effect of *Cx3cr1* deletion on the composition of the intestinal microbiota. Because the MCD diet is not physiological in terms of mimicking the metabolic situation during steatohepatitis development, we decided to continue with the HFD model for the analysis of the intestinal microbiota. Metagenomic DNA from cecal microbiome samples was used to generate amplicons of the V1-V3 hypervariable region of the 16S ribosomal RNA gene (rDNA) and sequenced using the 454 technology. Sixteen weeks of HFD resulted in marked alterations in both WT and *Cx3cr1*$^{-/-}$ mice, reflecting the microbial diversity within the individual groups (Fig. 3A; Supporting Fig. S3A,B). These results are also in line with the clustering according to genotype and diet in the principal coordinate analysis graph (Supporting Fig. S3C), indicating that HFD induced more pronounced changes in microbiota composition of *Cx3cr1*$^{-/-}$ mice compared to WT controls, which was also reflected by beta-diversity metrics (Supporting Fig. S3D).

To identify bacteria that define the key differences between the experimental groups, we computed a clustering analysis based on relative genus abundances. Interestingly, this analysis identified the bacterial genus *Akkermansia* as the defining bacteria for WT NCD mice, while *Bacteroides* was the major genus driving the partitioning in the *Cx3cr1*$^{-/-}$ HFD group (Fig. 3A). These data were confirmed by heatmap analysis, including the 40% most abundant genera (Supporting Fig. S4).

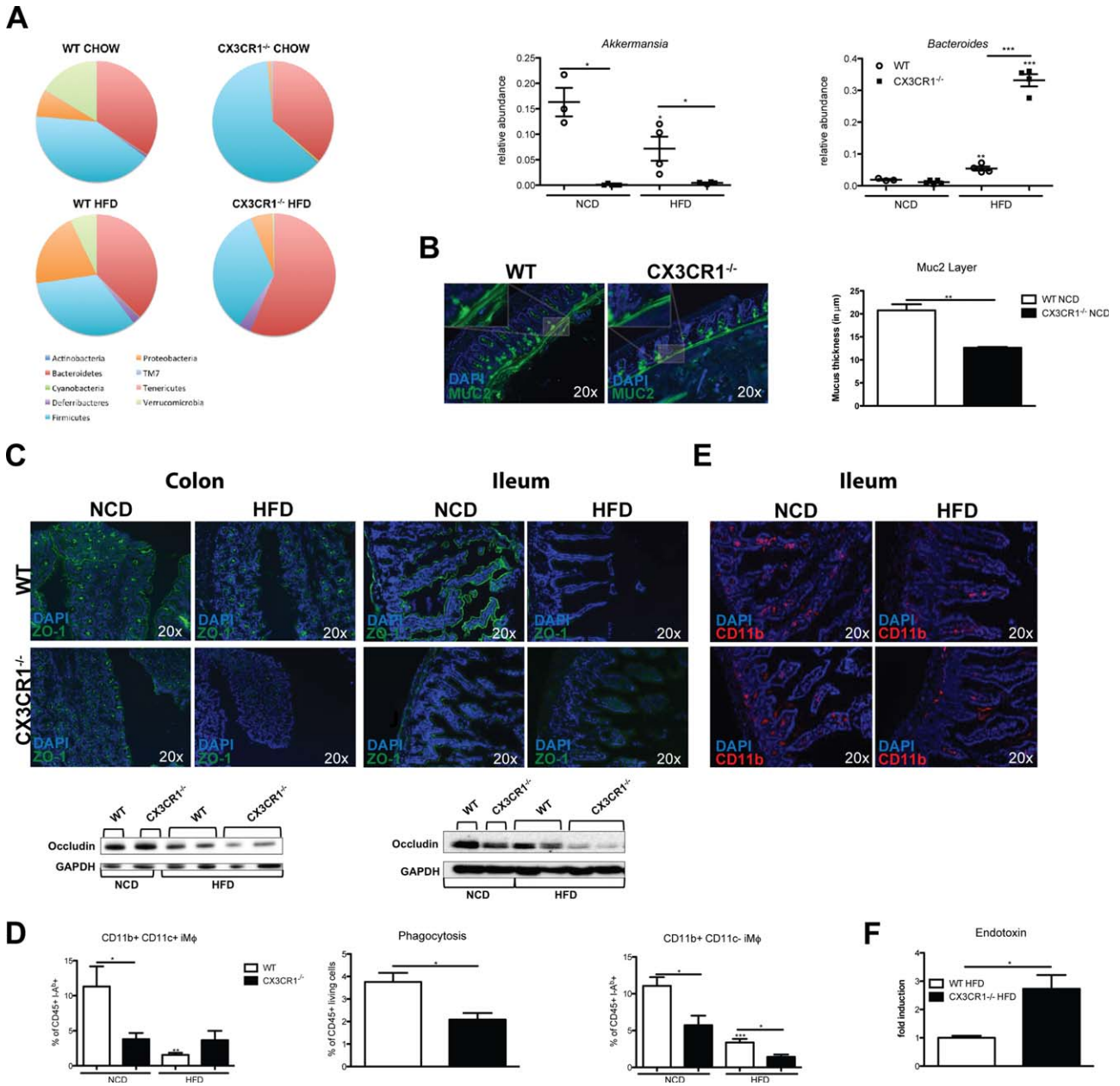

Fig. 3. Gut-microbiota composition and intestinal barrier integrity upon HFD. (A) Pie chart of multitag pyrosequencing data analyzed at the phylum level in WT and *Cx3cr1*$^{-/-}$ mice on NCD and HFD. Uncommon phyla that are a very small fraction of the total may not be visible in the chart even though they are present in the legend. Relative abundance of the bacterial genera *Akkermansia* and *Bacteroides* in WT and *Cx3cr1*$^{-/-}$ mice on NCD and HFD. (B) Immunofluorescent staining against Mucin-2 and quantification of the mucus thickness in colon samples of WT and *Cx3cr1*$^{-/-}$ mice. (C) Immunofluorescent staining and immunoblotting against the tight junction proteins zonula occludens 1 and occludin in colon and ileum of WT and *Cx3cr1*$^{-/-}$ mice. (D) Flow-cytometric analysis of colon lamina propria cells of the CD11b^{+}CD11c^{+} macrophage subset, phagocytic capacity, and the CD11b^{+}CD11c^{-} macrophage subset in WT and *Cx3cr1*$^{-/-}$ mice on NCD and HFD (gating strategy Supporting Fig. S4A). (E) Immunofluorescent staining against CD11b in ileum of WT and *Cx3cr1*$^{-/-}$ mice on NCD and HFD. (F) Portal endotoxin levels in WT and *Cx3cr1*$^{-/-}$ mice upon HFD. Data are expressed as the mean ± standard error of the mean and considered significant at $^{*}P < 0.05$, $^{**}P < 0.01$, and $^{***}P < 0.001$. *Significantly different from the resp. control group upon NCD, unless indicated differently. Abbreviations: DAPI, 4′,6-diamidino-2-phenylindole; GAPDH, glyceraldehyde 3-phosphate dehydrogenase; ZO-1, zonula occludens 1.

Because *Akkermansia muciniphila* is linked to intestinal barrier integrity and especially mucus production,[26,27] we evaluated the mucus layers in more detail. This analysis revealed that *Cx3cr1*$^{-/-}$ mice have thinner mucus layers in colon compared to WT mice (Fig. 3B). Additionally, HFD feeding led to reduced expression of the tight junction proteins zonula occludens 1 and occludin (Fig. 3C) in both ileum and colon of *Cx3cr1*$^{-/-}$ mice compared to WT controls. Together, these data indicate that CX3CR1 is involved in regulating intestinal barrier integrity.

Reduced Number of Intestinal Resident Macrophages and Increased Bacterial Translocation in Cx3cr1$^{-/-}$ Mice Upon HFD. Because resident macrophages in the gut (defined as CX3CR1^{hi}CD11b^{+} CD11c^{+}F4/80^{+}) have a gatekeeper function for the intestinal barrier, we analyzed colon lamina propria cells by FACS (gating strategy Supporting Fig. S5A). We observed basal differences in resident macrophages between WT and *Cx3cr1*$^{-/-}$ mice, which was associated with an overall decreased phagocytic capacity in *Cx3cr1*$^{-/-}$ mice (Fig. 3D). Furthermore, HFD induced a decrease in this specific macrophage subset in WT mice, while this did not further decrease in *Cx3cr1*$^{-/-}$ mice (Fig. 3D).

Additionally, CD11b^{+}CD11c^{-} macrophages were reduced in *Cx3cr1*$^{-/-}$ mice upon HFD compared to WT mice (Fig. 3D). These findings were confirmed by staining against CD11b, showing a reduction of CD11b^{+} cells in the ileum, which was more pronounced in *Cx3cr1*$^{-/-}$ mice upon HFD (Fig. 3E). In line with these findings, WT and *Cx3cr1*$^{-/-}$ mice showed decreased expression of tumor necrosis factor-alpha, *Mcp1*, and *Ccl5* in ileum after 16 weeks of HFD (Supporting Fig. S5B). These differences were also associated with changes in localization of CD11b^{+} cells in ileum. While CD11b^{+} cells had an equal distribution throughout the villi in WT mice upon HFD, these cells were mainly localized at the basement of the villi in *Cx3cr1*$^{-/-}$ mice (Fig. 3E). The observed phenotype was not due to a reduction of circulating Ly6C^{hi} classical monocytes (Supporting Fig. S5C), indicating that CX3CR1 mainly affects intestinal cell differentiation or recruitment.

Finally, to assess whether the impaired intestinal barrier also leads to higher translocation of PAMPs, we analyzed the endotoxin levels in portal vein serum from mice upon HFD. We found more endotoxin in *Cx3cr1*$^{-/-}$ mice compared to WT mice upon HFD (Fig. 3F), indicating increased translocation of bacterial products from the gut into the portal circulation.

CX3CR1 Can Regulate Innate Immune Signaling in Macrophages. Our data are consistent with an involvement of CX3CR1 in the maintenance of intestinal homeostasis and the physiological architecture of the lamina propria. To investigate the role of CX3CR1 signaling in macrophages in general, we prepared bone marrow–derived macrophages (BMDMs) of WT and *Cx3cr1*$^{-/-}$ mice. Resting BMDMs of *Cx3cr1*$^{-/-}$ mice displayed characteristics of preactivation, as shown by an elevated phagocytic capacity (Fig. 4A). Because resident intestinal macrophages are regularly exposed to high levels of PAMPs, we investigated the role of CX3CR1 in innate immune responses toward PAMPs. *Cx3cr1*$^{-/-}$ BMDMs released higher amounts of IL1β upon inflammasome stimulation (lipopolysaccharide + nigericin) compared to WT BMDMs (Fig. 4B). In addition, gene expression of *Nlrp3*, *Caspase 1*, and *Il1b* were increased in *Cx3cr1*$^{-/-}$ BMDMs upon inflammasome stimulation compared to WT BMDMs (Fig. 4C). By incubating NLRP3 macrophage reporter cells with CX3CL1 (FKN) before stimulation with nigericin, we observed that FKN suppressed inflammasome activation, which was also reflected by a decreased expression of IL1β in supernatant (Fig. 4D). Furthermore, WT and *Cx3cr1*$^{-/-}$ BMDMs released equal amounts of FKN in supernatant (Fig. 4E), and upon blocking FKN signaling with a neutralizing antibody WT and *Cx3cr1*$^{-/-}$ BMDMs showed an equal response to inflammasome stimulation (Fig. 4F). Hence, our *in vitro* experiments identified CX3CR1 as a regulator of the innate immune response through inflammasome signaling.

Administration of Broad-Spectrum Antibiotics Dampens Steatohepatitis and Restores Glucose Tolerance in Cx3cr1$^{-/-}$ Mice Upon HFD. Because *Cx3cr1*$^{-/-}$-derived BMDMs showed an aggravated response toward inflammasome stimulation, we tested whether eradication of the intestinal microbiota using broad-spectrum antibiotics had an impact on the progression of steatohepatitis. Antibiotic treatment in combination with HFD did not induce a difference in weight gain between WT and *Cx3cr1*$^{-/-}$ mice (Supporting Fig. S6E). However, antibiotic treatment significantly ameliorated steatohepatitis in *Cx3cr1*$^{-/-}$ mice to similar levels as WT mice (Fig. 5A), as indicated by an improved NAS, liver-to-body weight ratio, lower ALT levels, and a reduced number of CD45-positive cells (Supporting Fig. S6B). In addition, eradication of the intestinal microbiota improved hepatic steatosis (Fig. 5A,B) and glucose intolerance (Fig. 5C). Notably, *Cx3cr1*$^{-/-}$ mice had normal fasting glucose levels, suggesting that alterations in the microbial composition directly affect insulin resistance.

Antibiotic Treatment Dampens the Innate Immune Response in Cx3cr1$^{-/-}$ Mice and Affects Macrophage Polarization. We next investigated the effect of antibiotic treatment on the innate immune response in the liver. HFD significantly increased TLR4 protein and messenger RNA expression in WT and *Cx3cr1*$^{-/-}$ livers (Fig. 6A). Antibiotic treatment reduced TLR4 expression in both groups. Besides TLR4, HFD also induced the expression of *Nlrp3* and *Casp1*, which were significantly higher in *Cx3cr1*$^{-/-}$ mice compared to WT controls (Fig. 6B). In line with these findings, hepatic *Il1b* levels were also increased in *Cx3cr1*$^{-/-}$ mice upon HFD compared to WT controls (Fig. 6B).

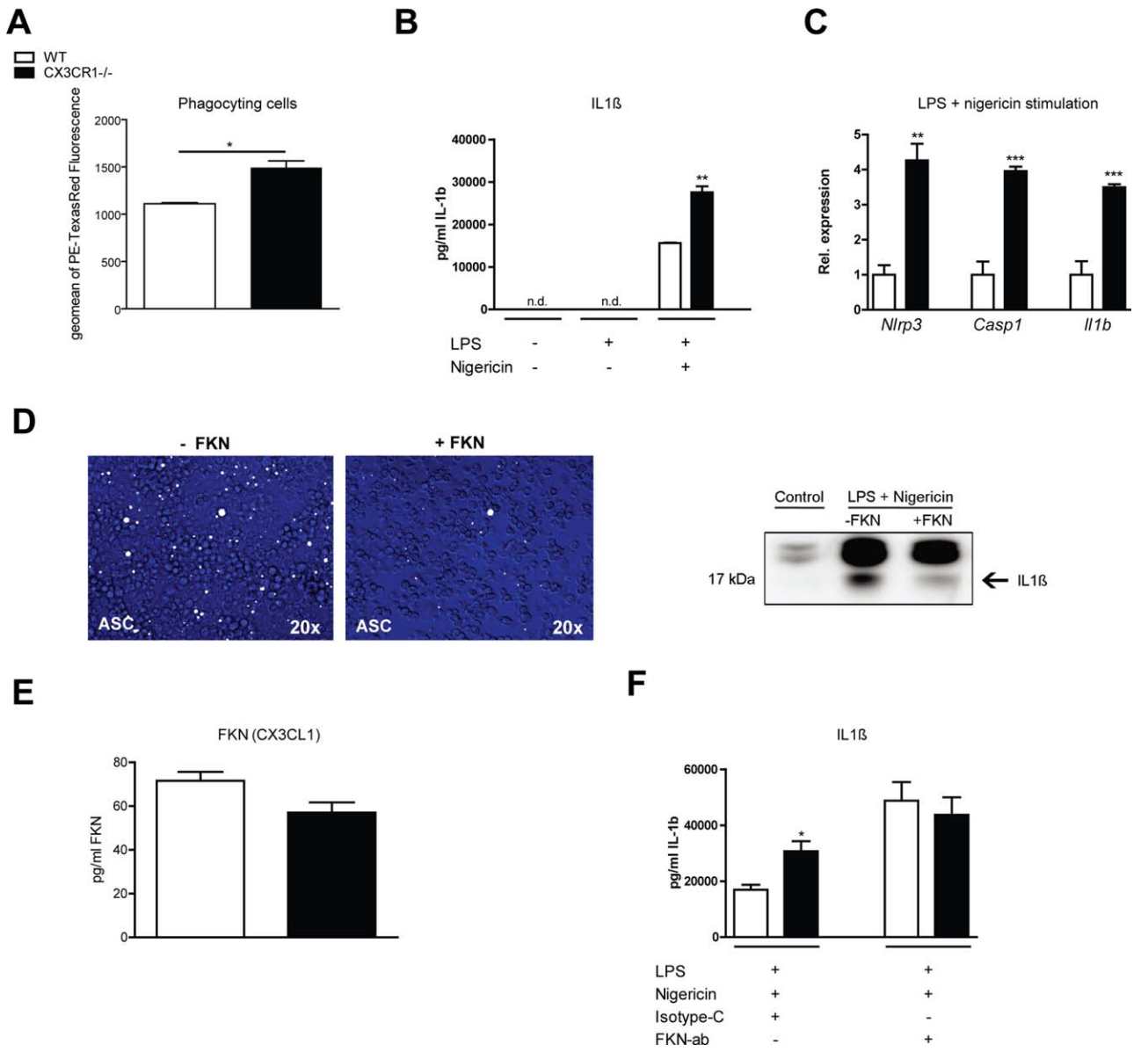

Fig. 4. Innate immune signaling in BMDMs. (A) Phagocytic capacity of WT and *Cx3cr1*$^{-/-}$ BMDMs. (B) Il1β levels in supernatant of WT and *Cx3cr1*$^{-/-}$ BMDMs upon inflammasome stimulation (LPS + nigericin). (C) Gene expression of *Nlrp3*, *Casp1*, and *Il1b* in BMDMs upon inflammasome stimulation (LPS + nigericin). (D) Inflammasome stimulation of macrophage reporter cells with and without FKN (0.03 nM) and immunoblotting of Il1β in supernatant of WT and *Cx3cr1*$^{-/-}$ BMDMs upon inflammasome stimulation with and without FKN (0.03 nM). (E) FKN levels in supernatant of WT and *Cx3cr1*$^{-/-}$ BMDMs. (F) Il1β levels in supernatant of WT and *Cx3cr1*$^{-/-}$ BMDMs upon inflammasome stimulation (LPS + nigericin) in combination with a CX3CL1 antibody or isotype control. Data are expressed as the mean ± standard error of the mean and considered significant at $*P < 0.05$, $**P < 0.01$, and $***P < 0.001$. *Significantly different from the resp. control group upon NCD, unless indicated differently. Abbreviations: LPS, lipopolysaccharide; PE, phycoerythrin; ASC, Apoptosis-associated speck-like protein containing a CARD.

Interestingly, antibiotic treatment was able to reduce the HFD-induced innate immune response in livers of *Cx3cr1*$^{-/-}$ mice (Fig. 6A,B).

Additionally, antibiotic treatment influenced the infiltration of CD11b^{+} inflammatory macrophages (Fig. 6C,D) and reduced the expression of *Mcp1* in livers of *Cx3cr1*$^{-/-}$ mice upon HFD (Fig. 6E). FACS analysis revealed that eradication of the intestinal microbiota dampened the infiltration of inflammatory CD11b^{hi}F4/80^{+} macrophages and induced a shift toward the "restorative" surface markers CD206^{+} and CD124^{+} on these cells (Fig. 6F). Altogether, these data suggest that intestinal dysbiosis in *Cx3cr1*$^{-/-}$ mice triggers activation of proinflammatory liver macrophages, thereby stimulating disease progression of steatohepatitis.

Discussion

The gut–liver axis plays an important role in the pathogenesis of chronic liver disease.[16,20] However, the

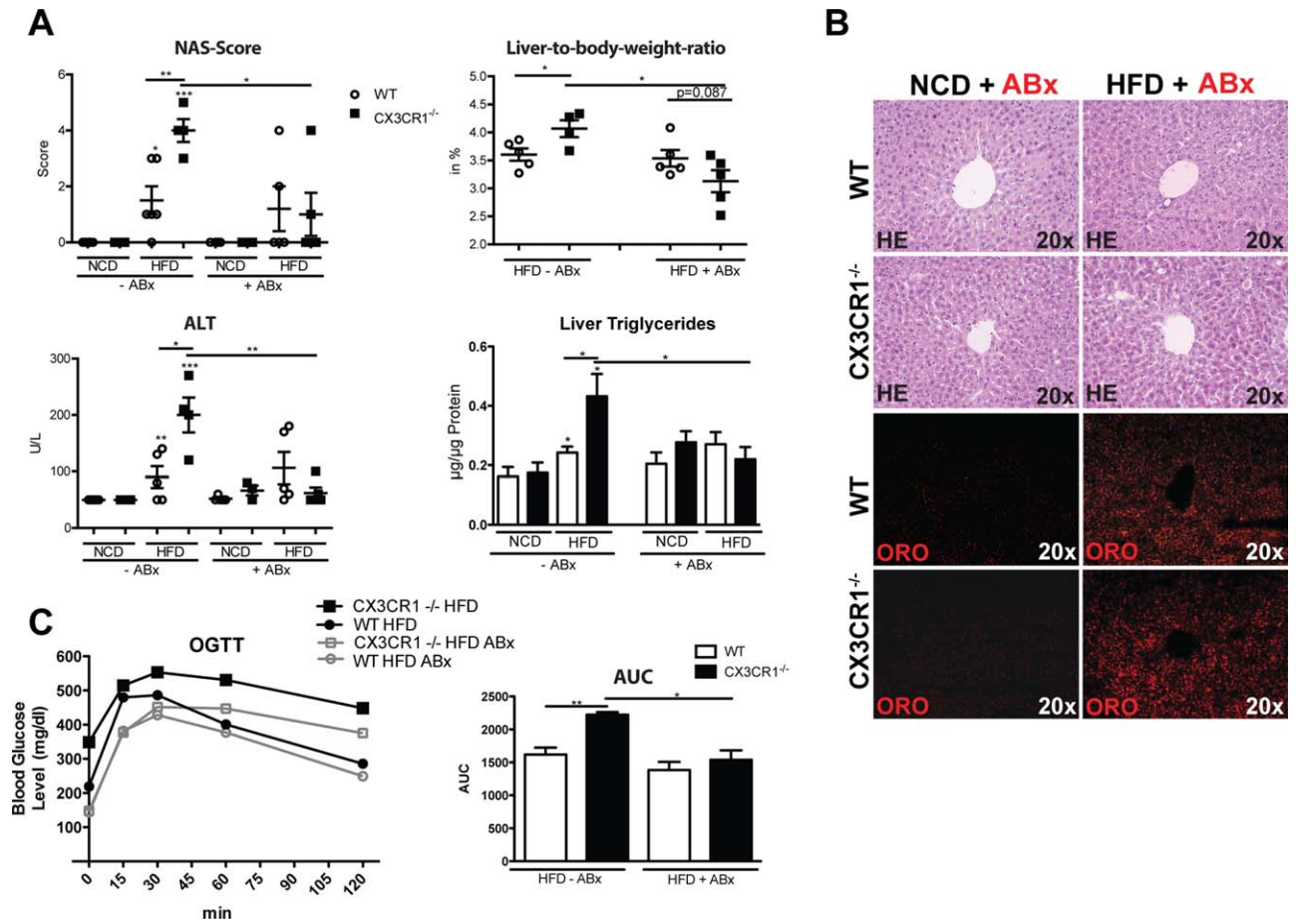

Fig. 5. The effect of broad-spectrum antibiotics on diet-induced steatohepatitis. (A) NAS, liver-to-body weight ratio, serum ALT levels, and hepatic triglyceride levels in WT and *Cx3cr1*$^{-/-}$ mice on NCD and HFD, with and without antibiotic treatment. (B) Hematoxylin and eosin and oil red O staining for lipid accumulation. (C) Oral glucose tolerance test and area under the curve after 0, 15, 30, 60, and 120 minutes. (NCD and HFD groups without antibiotic treatment are similar to Fig. 1). Data are expressed as the mean ± standard error of the mean and considered significant at $*P < 0.05$, $**P < 0.01$, and $***P < 0.001$, respectively. *Significantly different from the resp. control group upon NCD, unless indicated differently. Abbreviations: ABx, antibiotics; AUC, area under the curve; HE, hematoxylin and eosin; OGTT, oral glucose tolerance test; ORO, oil red O.

exact contribution of the intestinal barrier and dysbiosis to steatohepatitis pathogenesis and its potential therapeutic implications remain unclear.[28] In the current study, we investigated the contribution of CX3CR1 in controlling gut–liver interactions during progression of diet-induced steatohepatitis. We demonstrated that CX3CR1 signaling is crucial in the maintenance of intestinal homeostasis during steatohepatitis by maintaining intestinal barrier integrity. Therefore, our data identified CX3CR1 as a gatekeeper of steatohepatitis.

The concept that intestinal inflammation acts as an important driver for liver diseases was initially inspired by observations in patients suffering from inflammatory bowel disease, who often present elevated transaminases.[29,30] Interestingly, the two single-nucleotide polymorphisms (T280M and V249I) in the coding sequence of *CX3CR1*, which confers functionally reduced binding of FKN to its receptor, have been associated with Crohn's disease, suggesting more inflammatory activities.[31] These findings indicate that a dysregulated CX3CR1–FKN axis contributes to disease progression. Importantly, steatohepatitis is associated with a leaky gut and intestinal dysbiosis.[18,32] However, these studies could not answer the question of whether an impaired intestinal barrier is a cause or a consequence. In the present study, we showed that loss of *Cx3cr1* renders mice more susceptible toward HFD-induced liver injury, which was triggered by loss of intestinal barrier integrity.

CX3CR1 is an important regulator of intestinal macrophage homeostasis,[14] which is in line with our observations that the intestinal macrophage populations in WT and *Cx3cr1*$^{-/-}$ mice are different. Similar to observations in dextran sodium sulfate colitis,[33] HFD led to a reduction of $CD11b^{+}CD11c^{+}$ resident macrophages. These macrophages have a high phagocytic capacity and have gatekeeper functions in the intestinal lamina

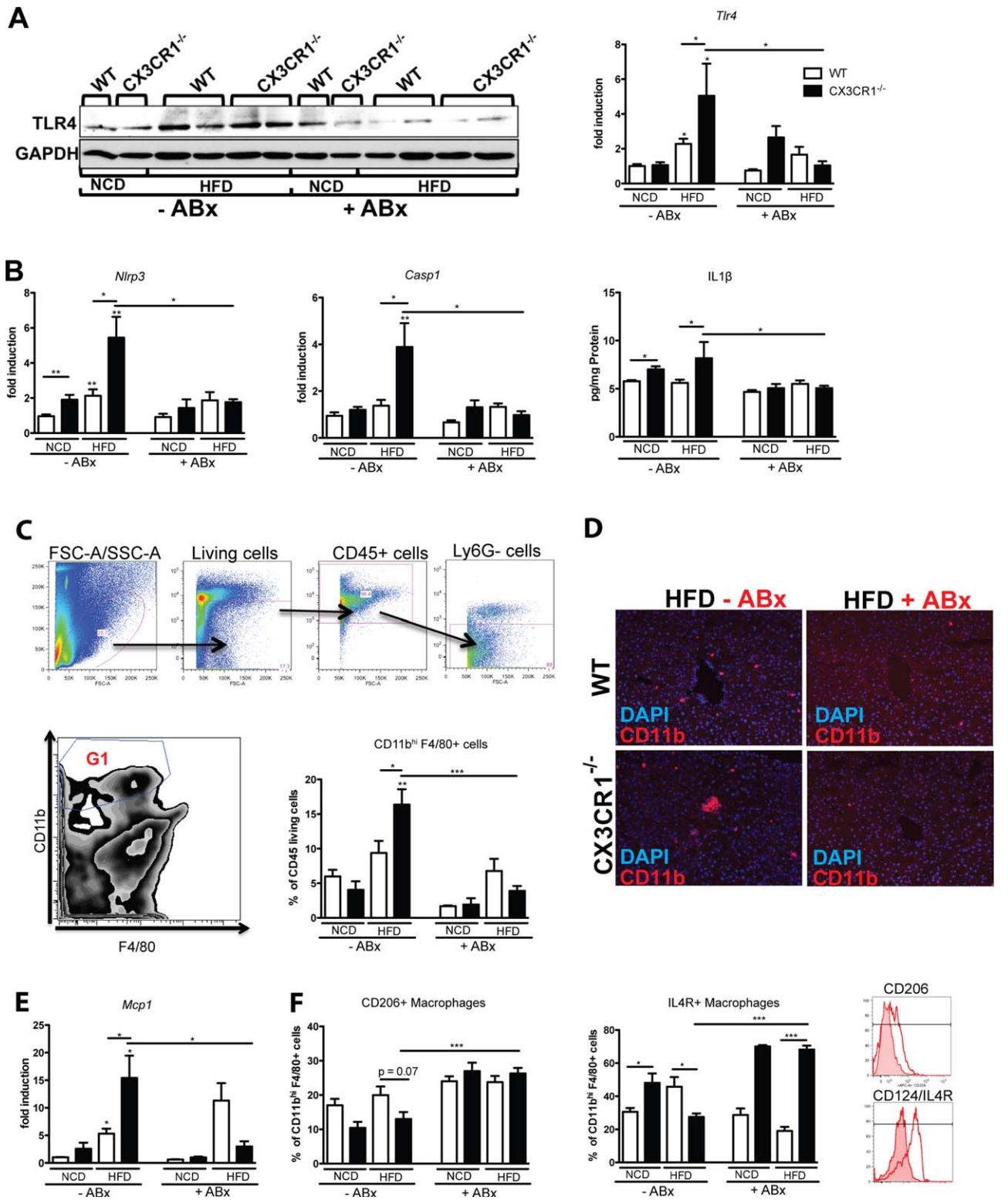

Fig. 6. The hepatic innate immune response upon antibiotic treatment. (A) TLR4 immunoblotting and gene expression in livers of WT and *Cx3cr1*$^{-/-}$ mice on NCD and HFD, with and without antibiotic treatment. (B) Hepatic gene expression of the inflammasome components *Nlrp3* and *Casp1* and cytokine levels of IL1β in whole-liver lysates of WT and *Cx3cr1*$^{-/-}$ mice. (C) Flow-cytometric analysis of the infiltrating inflammatory macrophages (CD11b^{hi}F4/80^{low}) in livers of WT and *Cx3cr1*$^{-/-}$ mice. (D) Immunofluorescent staining against CD11b in livers of WT and *Cx3cr1*$^{-/-}$ mice on HFD, with and without antibiotic treatment. (E) Hepatic gene expression of *Mcp1*. (F) Flow-cytometric analysis of the "restorative" surface markers CD206^{+} and CD124^{+} on the CD11b^{hi}F4/80^{low} macrophages. (NCD and HFD groups without antibiotic treatment are similar to Fig. 2.) Data are expressed as the mean $\pm$ standard error of the mean and considered significant at $^{*}P < 0.05$, $^{**}P < 0.01$, and $^{***}P < 0.001$, respectively. *Significantly different from the resp. control group upon NCD, unless indicated differently. Abbreviations: ABx, antibiotics; DAPI, 4′,6-diamidino-2-phenylindole; FSC-A, forward scatter-area; GAPDH, glyceraldehyde 3-phosphate dehydrogenase; SSC-A, side scatter-area.

propria, thereby limiting translocation of PAMPs to the portal vein.[34] As these macrophages are the main source of tumor necrosis factor,[35] the reduced tumor necrosis factor levels in our study are most likely a result of the reduction in this protective macrophage subset. Collectively, a balanced milieu between proinflammatory and anti-inflammatory stimuli is necessary for intestinal homeostasis, thereby maintaining the physiological mononuclear phagocyte subsets and barrier integrity.

One hallmark of intestinal macrophages is a profound inflammatory anergy toward PAMPs.[36] Because we observed marked differences in macrophage number and distribution in the intestine upon HFD, we investigated the role of CX3CR1 signaling in macrophages in general. Our *in vitro* data in BMDMs revealed that blocking *Cx3cr1* sensitizes macrophages to inflammasome activation. Recent data also indicate that inflammasome activation is linked to NASH progression.[37,38] In contrast to these findings, Henao-Mejia et al. demonstrated that inflammasome activation can negatively regulate NASH progression through alterations in the gut microbiota.[39] Furthermore, inflammasome activation is also able to regulate intestinal homeostasis during dextran sodium sulfate–induced colitis and goblet cell mucus secretion in mice, thereby protecting the intestinal integrity and making cells sensitive for clearance of enteric pathogens from the mucosal surface.[40-42] Together, these data demonstrate that a tight regulation of inflammasome-mediated innate immunity plays an important role in intestinal homeostasis and that CX3CR1 is an essential gatekeeper in controlling this process.

Besides being the central organ of metabolism, the liver is also the first site that encounters PAMPs through the portal circulation. Therefore, the liver is particularly enriched with innate immune cells, which points toward a role of CX3CR1 in mediating the innate immune response upon metabolic disorders. Recent findings showed that *Cx3cr1*$^{-/-}$ mice had less glucose intolerance after 10 weeks of HFD, which was attributed to reduced white adipose tissue inflammation, a major cause of insulin resistance.[43] In contrast, Lee et al. found that *Cx3cr1*$^{-/-}$ mice were more prone to develop glucose intolerance after 16 weeks of HFD feeding,[5] which is also supported by our findings, demonstrating that *Cx3cr1*$^{-/-}$ mice have higher fasting glucose levels and stronger glucose intolerance compared to WT mice. These contradictory data regarding glucose intolerance in *Cx3cr1*$^{-/-}$ mice might be attributed to differences in intestinal microbiota composition. Our microbiota analysis revealed that *Cx3cr1*$^{-/-}$ mice on HFD showed a pattern that was recently linked to insulin resistance[44]—overgrowth of *Bacteroides* and reduction of *Akkermansia muciniphila*.

The gut–liver crosstalk in our study also suggested a pronounced pathogen recognition receptor–mediated inflammatory response. Similarly, it has been demonstrated that TLR4-mediated hepatic inflammation can suppress insulin signaling by inhibiting AKT phosphorylation.[45] Therefore, alterations in microbiota composition and hepatic inflammation might explain the susceptibility and/or progression toward insulin resistance in *Cx3cr1*$^{-/-}$ mice. In line with these findings, antibiotic treatment abrogated the inflammatory response in our *Cx3cr1*$^{-/-}$ mice upon HFD and led to improved glucose tolerance. Because inflammasome activation is highlighted in multiple manifestations of the metabolic syndrome,[46] it was demonstrated that NLRP3-mediated release of IL1β is promoting insulin resistance,[47,48] beta-cell death,[49] and atherosclerotic plaque formation.[50] Collectively, these data indicate that inflammasome regulation through CX3CR1 and gut–liver interactions are central for the development of the metabolic syndrome.

In summary, our data demonstrate the functional relevance of the CX3CR1–FKN axis in the pathogenesis of NASH (Supporting Fig. S7). CX3CR1 limits the progression of steatohepatitis and the onset of glucose intolerance by maintaining intestinal barrier integrity. Strikingly, this effect was dependent on the intestinal microbiota composition as antibiotic treatment could rescue the NASH phenotype in *Cx3cr1*$^{-/-}$ mice. Our study extends the growing knowledge about the central role of various chemokines in the pathogenesis of NASH. We identified the chemokine receptor CX3CR1 as a gatekeeper of diet-induced steatohepatitis by maintaining intestinal homeostasis. Therefore, future studies are warranted to assess the potential modulation of chemokines and their receptors to treat patients with NASH. Hence, our data identified CX3CR1 as a gatekeeper and potential therapeutic target of diet-induced steatohepatitis.

References

1. Schattenberg JM, Schuppan D. Nonalcoholic steatohepatitis: the therapeutic challenge of a global epidemic. Curr Opin Lipidol 2011;22:479-488.
2. Vernon G, Baranova A, Younossi ZM. Systematic review: the epidemiology and natural history of non-alcoholic fatty liver disease and non-alcoholic steatohepatitis in adults. Aliment Pharmacol Ther 2011;34:274-285.
3. Law K, Brunt EM. Nonalcoholic fatty liver disease. Clin Liver Dis 2010;14:591-604.
4. Dowman JK, Tomlinson JW, Newsome PN. Pathogenesis of non-alcoholic fatty liver disease. QJM 2010;103:71-83.

5. Lee YS, Morinaga H, Kim JJ, Lagakos W, Taylor S, Keshwani M, et al. The fractalkine/CX3CR1 system regulates beta cell function and insulin secretion. Cell 2013;153:413-425.
6. Xueyao Y, Saifei Z, Dan Y, Qianqian P, Xuehong D, Jiaqiang Z, et al. Circulating fractalkine levels predict the development of the metabolic syndrome. Int J Endocrinol 2014;2014:715148.
7. Combadiere C, Potteaux S, Gao JL, Esposito B, Casanova S, Lee EJ, et al. Decreased atherosclerotic lesion formation in CX3CR1/apolipoprotein E double knockout mice. Circulation 2003;107:1009-1016.
8. Tacke F, Alvarez D, Kaplan TJ, Jakubzick C, Spanbroek R, Llodra J, et al. Monocyte subsets differentially employ CCR2, CCR5, and CX3CR1 to accumulate within atherosclerotic plaques. J Clin Invest 2007;117:185-194.
9. Serino M, Blasco-Baque V, Nicolas S, Burcelin R. Far from the eyes, close to the heart: dysbiosis of gut microbiota and cardiovascular consequences. Curr Cardiol Rep 2014;16:540.
10. Tremaroli V, Backhed F. Functional interactions between the gut microbiota and host metabolism. Nature 2012;489:242-249.
11. Sanz Y, Olivares M, Moya-Perez A, Agostoni C. Understanding the role of gut microbiome in metabolic disease risk. Pediatr Res 2015;77: 236-244.
12. Zigmond E, Jung S. Intestinal macrophages: well educated exceptions from the rule. Trends Immunol 2013;34:162-168.
13. Niess JH, Brand S, Gu X, Landsman L, Jung S, McCormick BA, et al. CX3CR1-mediated dendritic cell access to the intestinal lumen and bacterial clearance. Science 2005;307:254-258.
14. Medina-Contreras O, Geem D, Laur O, Williams IR, Lira SA, Nusrat A, et al. CX3CR1 regulates intestinal macrophage homeostasis, bacterial translocation, and colitogenic Th17 responses in mice. J Clin Invest 2011;121:4787-4795.
15. Brand S, Sakaguchi T, Gu X, Colgan SP, Reinecker HC. Fractalkine-mediated signals regulate cell-survival and immune-modulatory responses in intestinal epithelial cells. Gastroenterology 2002;122:166-177.
16. Ilan Y. Leaky gut and the liver: a role for bacterial translocation in nonalcoholic steatohepatitis. World J Gastroenterol 2012;18:2609-2618.
17. Schnabl B, Brenner DA. Interactions between the intestinal microbiome and liver diseases. Gastroenterology 2014;146:1513-1524.
18. Miele L, Valenza V, La Torre G, Montalto M, Cammarota G, Ricci R, et al. Increased intestinal permeability and tight junction alterations in nonalcoholic fatty liver disease. Hepatology 2009;49:1877-1887.
19. Johansson ME, Phillipson M, Petersson J, Velcich A, Holm L, Hansson GC. The inner of the two Muc2 mucin-dependent mucus layers in colon is devoid of bacteria. Proc Natl Acad Sci USA 2008; 105:15064-15069.
20. Schnabl B. Linking intestinal homeostasis and liver disease. Curr Opin Gastroenterol 2013;29:264-270.
21. Friedman SL. Liver fibrosis in 2012: convergent pathways that cause hepatic fibrosis in NASH. Nat Rev Gastroenterol Hepatol 2013;10:71-72.
22. Jung S, Aliberti J, Graemmel P, Sunshine MJ, Kreutzberg GW, Sher A, et al. Analysis of fractalkine receptor CX(3)CR1 function by targeted deletion and green fluorescent protein reporter gene insertion. Mol Cell Biol 2000;20:4106-4114.
23. **Hatting M**, **Zhao G**, Schumacher F, Sellge G, Al Masaoudi M, Gabetaler N, et al. Hepatocyte caspase-8 is an essential modulator of steatohepatitis in rodents. Hepatology 2013;57:2189-2201.
24. **Kroy DC**, **Schumacher F**, Ramadori P, Hatting M, Bergheim I, Gassler N, et al. Hepatocyte specific deletion of c-Met leads to the development of severe non-alcoholic steatohepatitis in mice. J Hepatol 2014;61:883-890.
25. Bieghs V, Trautwein C. The innate immune response during liver inflammation and metabolic disease. Trends Immunol 2013;34:446-452.
26. Everard A, Belzer C, Geurts L, Ouwerkerk JP, Druart C, Bindels LB, et al. Cross-talk between *Akkermansia muciniphila* and intestinal epithelium controls diet-induced obesity. Proc Natl Acad Sci USA 2013;110: 9066-9071.
27. Derrien M, Vaughan EE, Plugge CM, de Vos WM. *Akkermansia muciniphila* gen. nov., sp. nov., a human intestinal mucin-degrading bacterium. Int J Syst Evol Microbiol 2004;54:1469-1476.
28. Chassaing B, Etienne-Mesmin L, Gewirtz AT. Microbiota–liver axis in hepatic disease. Hepatology 2014;59:328-339.
29. Wewer V, Gluud C, Schlichting P, Burcharth F, Binder V. Prevalence of hepatobiliary dysfunction in a regional group of patients with chronic inflammatory bowel disease. Scand J Gastroenterol 1991;26: 97-102.
30. Broome U, Glaumann H, Hellers G, Nilsson B, Sorstad J, Hultcrantz R. Liver disease in ulcerative colitis: an epidemiological and follow up study in the county of Stockholm. Gut 1994;35:84-89.
31. **Brand S**, **Hofbauer K**, Dambacher J, Schnitzler F, Staudinger T, Pfennig S, et al. Increased expression of the chemokine fractalkine in Crohn's disease and association of the fractalkine receptor T280M polymorphism with a fibrostenosing disease phenotype. Am J Gastroenterol 2006;101:99-106.
32. Wigg AJ, Roberts-Thomson IC, Dymock RB, McCarthy PJ, Grose RH, Cummins AG. The role of small intestinal bacterial overgrowth, intestinal permeability, endotoxaemia, and tumour necrosis factor alpha in the pathogenesis of non-alcoholic steatohepatitis. Gut 2001;48:206-211.
33. Bain CC, Scott CL, Uronen-Hansson H, Gudjonsson S, Jansson O, Grip O, et al. Resident and pro-inflammatory macrophages in the colon represent alternative context-dependent fates of the same Ly6Chi monocyte precursors. Mucosal Immunol 2013;6:498-510.
34. Bain CC, Mowat AM. Macrophages in intestinal homeostasis and inflammation. Immunol Rev 2014;260:102-117.
35. **Zigmond E**, **Varol C**, Farache J, Elmaliah E, Satpathy AT, Friedlander G, et al. Ly6C hi monocytes in the inflamed colon give rise to proinflammatory effector cells and migratory antigen-presenting cells. Immunity 2012;37:1076-1090.
36. Smythies LE, Sellers M, Clements RH, Mosteller-Barnum M, Meng G, Benjamin WH, et al. Human intestinal macrophages display profound inflammatory anergy despite avid phagocytic and bacteriocidal activity. J Clin Invest 2005;115:66-75.
37. Wree A, Eguchi A, McGeough MD, Pena CA, Johnson CD, Canbay A, et al. NLRP3 inflammasome activation results in hepatocyte pyroptosis, liver inflammation, and fibrosis in mice. Hepatology 2014;59: 898-910.
38. Wree A, McGeough MD, Pena CA, Schlattjan M, Li H, Inzaugarat ME, et al. NLRP3 inflammasome activation is required for fibrosis development in NAFLD. J Mol Med (Berl) 2014;92:1069-1082.
39. **Henao-Mejia J**, **Elinav E**, **Jin C**, Hao L, Mehal WZ, Strowig T, et al. Inflammasome-mediated dysbiosis regulates progression of NAFLD and obesity. Nature 2012;482:179-185.
40. Wlodarska M, Thaiss CA, Nowarski R, Henao-Mejia J, Zhang JP, Brown EM, et al. NLRP6 inflammasome orchestrates the colonic host-microbial interface by regulating goblet cell mucus secretion. Cell 2014;156:1045-1059.
41. **Elinav E**, **Strowig T**, Kau AL, Henao-Mejia J, Thaiss CA, Booth CJ, et al. NLRP6 inflammasome regulates colonic microbial ecology and risk for colitis. Cell 2011;145:745-757.
42. Zaki MH, Boyd KL, Vogel P, Kastan MB, Lamkanfi M, Kanneganti TD. The NLRP3 inflammasome protects against loss of epithelial integrity and mortality during experimental colitis. Immunity 2010;32: 379-391.
43. Polyak A, Ferenczi S, Denes A, Winkler Z, Kriszt R, Pinter-Kubler B, et al. The fractalkine/Cx3CR1 system is implicated in the development of metabolic visceral adipose tissue inflammation in obesity. Brain Behav Immun 2014;38:25-35.
44. Suez J, **Korem T**, **Zeevi D**, **Zilberman-Schapira G**, Thaiss CA, Maza O, et al. Artificial sweeteners induce glucose intolerance by altering the gut microbiota. Nature 2014;514:181-186.

45. Shi H, Kokoeva MV, Inouye K, Tzameli I, Yin H, Flier JS. TLR4 links innate immunity and fatty acid–induced insulin resistance. J Clin Invest 2006;116:3015-3025.
46. Esser N, Legrand-Poels S, Piette J, Scheen AJ, Paquot N. Inflammation as a link between obesity, metabolic syndrome and type 2 diabetes. Diabetes Res Clin Pract 2014;105:141-150.
47. Vandanmagsar B, Youm YH, Ravussin A, Galgani JE, Stadler K, Mynatt RL, et al. The NLRP3 inflammasome instigates obesity-induced inflammation and insulin resistance. Nat Med 2011;17:179-188.
48. Wen H, Gris D, Lei Y, Jha S, Zhang L, Huang MT, et al. Fatty acid–induced NLRP3-ASC inflammasome activation interferes with insulin signaling. Nat Immunol 2011;12:408-415.
49. Masters SL, Dunne A, Subramanian SL, Hull RL, Tannahill GM, Sharp FA, et al. Activation of the NLRP3 inflammasome by islet amyloid polypeptide provides a mechanism for enhanced IL-1beta in type 2 diabetes. Nat Immunol 2010;11:897-904.
50. **Duewell P**, **Kono H**, Rayner KJ, Sirois CM, Vladimer G, Bauernfeind FG, et al. NLRP3 inflammasomes are required for atherogenesis and activated by cholesterol crystals. Nature 2010;464:1357-1361.

Author names in bold designate shared co-first authorship.

Supporting Information

Additional Supporting Information may be found at onlinelibrary.wiley.com/doi/10.1002/hep.27982/suppinfo.